ELSEVIER

Journal of Nuclear Materials 241–243 (1997) 1203–1209

journal of nuclear materials

Applications of superpermeable membranes in fusion: The flux density problem and experimental progress

A. Livshits [a,*], N. Ohyabu [b], M. Notkin [a], V. Alimov [a], H. Suzuki [b], A. Samartsev [a], M. Solovyov [a], I. Grigoriadi [a], A. Glebovsky [a], A. Busnyuk [a], A. Doroshin [a], K. Komatsu [b]

[a] *Bonch-Bruyevich University, 61 Moika, 191186 St. Petersburg, Russia*
[b] *National Institute for Fusion Science, Furoh-cho, Chikusa-ku, Nagoya 464-01, Japan*

Abstract

Superpermeable membranes whose permeability to energetic hydrogen approaches the permeability of an opening of the same area can be employed to separate D/T and He in fusion machine exhausts, to control the edge plasma and divertor conditions (by pumping and/or arranging of gas circulation through SOL or divertor) and to pump and recuperate D/T in auxiliary systems e.g. in pellet or neutral beam injection. One of the key points is the operation at permeation flux densities of up to 10^{16}–10^{19} cm^{-2} s^{-1}. Theory predicts that the highest flux densities may be reached with superpermeable membranes based on the *V group* metals: the limit conditioned by a maximum permissible hydrogen concentration in bulk metal is expected to be as high as $\sim 10^{19}$ cm^{-2} s^{-1}. The experimental membrane system comprised a cylindrical Nb membrane and an incandescent Ta/Nb atomizer placed inside. The hydrogen pumping speed by this system amounts to $\sim 10^3$ l/s, with a specific pumping speed of ~ 1 l/s per cm^2 membrane area and ~ 8 l/s per cm^2 atomizer area. Superpermeability was observed at record parameters referring both to the flux density of 3×10^{17} $H/cm^2/s$ (by one order of magnitude larger than ever before) and to the operational pressure of 3×10^{-2} Torr. A long-term reliable operation of this system proved being possible even in a vacuum far inferior to UHV conditions.

Keywords: Active pumping; Fusion technology

1. Introduction

1.1. Superpermeability

Metal membranes may be superpermeable to the suprathermal hydrogen particles whose energy (kinetic, internal or chemical) exceeds ~ 1 eV [1,2]. The term *superpermeability* has been suggested to indicate that the permeability of a membrane approaches the maximum conceivable limit: the permeability of an opening of the same area. Superpermeability to thermal hydrogen atoms and to fast ions was observed on membranes of Ni [3], Fe [4,5], Pd [2,6,7] and Nb [2,8–11]. The hydrogen that passes through superpermeable membranes is automatically compressed and purged of all impurities, including He.

The barrier for the dissociative absorption of hydrogen molecules at the membrane inlet surface is responsible for the phenomenon [1,2]. Such barriers typically appear due to the presence of *monatomic non-metal films* at a metal surface [2–4,6–11]. The thin non-metallic overlayers exhibit a highly selective permeability to suprathermal hydrogen, thus

* Corresponding author. Tel.: +7-812 314 6659; fax: +7-812 315 7610 or +7-812 314 3360; e-mail: samar@qrel.sut.ru.

PII S0022-3115(96)00700-3

inhibiting both the back release of the incoming particles that 'cool down' in the metal lattice and the back permeation of molecular hydrogen evolved at the downstream side. A membrane with symmetric surfaces may let through a half of the flux absorbed, and virtually the whole incoming flux may pass, if the evolution is easier at the downstream surface [1,2,6]. It is important that a metal surface covered with nearly monatomic non-metal layers (a 'real' surface) is thermodynamically stable and it reveals a remarkable capability for self-maintenance under the action of a wide variety of agents [10]. In particular, it may be absolutely stable under *thermal atomic hydrogen* despite its known chemical activity [2–4,6,8–11]. In addition, the non-metallic films effectively protect bulk metal from chemically active gas impurities.

Typically, metal surfaces subjected to routine cleaning procedures and heated at moderate temperatures in vacuum are covered with non-metallic films of about a monolayer thickness strongly bound at the surface, whereas thicker non-metal layers either get evaporated, or get dissolved in bulk metal [12]. One can expect for the above reasons that a stable long-term operation of superpermeable membranes may be possible under realistic fusion device conditions, even though superpermeability is governed by rather delicate interphase processes.

1.2. Possible applications in fusion and the flux densities required

Superpermeable membranes may be employed: (1) for the *separation of D / T fuel and He ashes in fusion device exhausts*, with the aim of decreasing tritium accumulation and thus improving safety, (2) for controlling of the edge plasma and divertor conditions by pumping and arranging of *gas circulation through SOL or divertor*, and (3) for *pumping and recuperation of D / T in auxiliary systems* (pellet and neutral beam injectors, etc.).

For instance, superpermeable membranes were suggested [10,11] to be installed in the ITER pumping ducts in order to isolate D/T and substantially reduce the tritium load on the cryogenic pumps serving for helium evacuation. One option is to place the membranes at some distance from the divertor where the D/T gas is already thermalized, with suprathermal hydrogen being generated e.g. at a hot metal surface specially introduced to atomize D/T. Corresponding model experiments with both the membranes and incandescent atomizers made of *V group* metals were carried out [10,11]. According to our estimates [10], 90 to 99.9% of D/T (depending on the cryopump pumping speed [13]) can be isolated with membrane systems occupying $\sim$ 1.5 m length of every ITER duct. The D/T isolated and compressed by the membranes can be either returned into the fuelling system or, at least partly, directed back into the divertor to control its gas dynamics regimes [11]. In the former case, a permeation flux density $\leq 3 \times 10^{16}$ atom/s *per* cm^2 membrane area will be sufficient (a value already obtained experimentally [7,10]), but in the latter case the flux required is substantially (10 times or more) higher.

Another example is the proposal to employ the membrane pumping in the large helical device (LHD) under construction in Japan now. Specifically, the suggestion is to evacuate hydrogen out of the LHD divertor with a maximum possible speed in order to provide for the high-temperature divertor plasma operation [14], which is supposed to permit temperature enhancement of the main plasma. Our evaluations yield flux densities of 10^{16}–10^{17} atom/cm^2/s required for a helical divertor, while fluxes of up to 10^{18}–10^{19} will be necessary for a more compact 'local island divertor' [14].

1.3. Upper limit of the flux density at superpermeability

There is a number of mechanisms [2,9] that degrade superpermeability with the permeation flux density rising: (1) thermal re-emission of absorbed atoms through their recombinative release at the surface, (2) re-emission induced by incident energetic particles and (3) degradation of the surface and of the subsurface area under the action of energetic hydrogen, including the destruction of the surface barrier through sputtering of non-metallic overlayers. Rough estimates still permit the conclusion [10] that none of the above mechanisms should put limitations on the flux density for membranes based on the *V group metals* acted upon by *thermal atomic hydrogen*. The main limiting factor in this case will be a maximum permissible concentration of hydrogen in the metal lattice. If we take 5 at% of H as a value not to exceed, we get rather a high achievable flux density of $\sim 10^{19}$ cm^{-2} s^{-1} [10]. However, only fluxes of $< 3 \times 10^{16}$ cm^{-2} s^{-1} have been obtained experimentally up to date [7,10].

2. Experiment

The membrane system design resembled to a great degree that proposed for ITER and tested in our previous experiments [10,11]. It is a combination of a membrane and an atomizer directly facing one another, both made of *V group* metals.

A cylindrical *membrane* of 12.5 cm diameter and 25 cm length ($\sim$ 1000 cm^2 area), made of a 100 μm-thick Nb foil, is mounted along the walls of a vacuum vessel (Fig. 1). A set of 1.5 mm-thick resistively heated Ta wires serves as an *atomizer* of molecular hydrogen. Its full surface area is 200 cm^2 i.e. 20% of the membrane (making a larger atomizer would

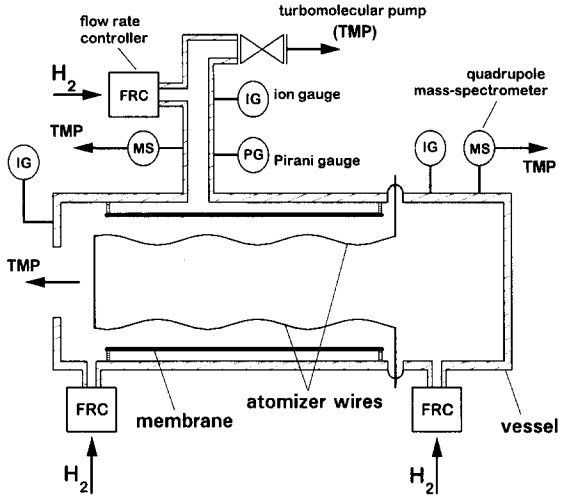

Fig. 1. Schematic of the experimental apparatus.

be of little advantage, since the atomizer efficiency ceases to grow with the degree of atomization approaching unity and only few non-atomized molecules hitting the atomizer). In these experimental series, only one atomizer section of 125 cm^2 area was employed.

The membrane temperature is determined by the balance of the radiation heating from the atomizer and of the heat removal by radiation to the water-cooled vessel. Piezo-electric flow rate controllers/meters are employed to admit hydrogen and to calibrate permeation flux measurements. (Such a calibration is important to correctly measure the *permeation flux*, J_m, irrespective of the changes in pumping speed, in gauge sensitivity, and in the gas flow regimes in downstream connection tubes due to changes in J_m and the downstream pressure.) The pumping speed by the membrane, S_m, can be computed as:

$$S_m\,(\mathrm{l/s}) = J_m\,(\mathrm{molecule/s})/p\,(\mathrm{Torr})/3.3\times 10^{19}. \tag{1}$$

Two turbo-molecular pumps, of 2000 and 500 l/s speed, pump the vacuum chambers at the upstream and downstream sides of the membrane, respectively. The membrane assembly itself is a bakeable UHV system, but it is mounted into a linear plasma machine (plasma–membrane experiments are planned for the future) that is unbakeable and is greased with oil. Correspondingly, we could not get a *background pressure* lower than 5×10^{-7} Torr, with H_2O and organic impurities being the main ambient gases. All the previous superpermeation experiments were carried out with UHV oil-free systems (though chemically active impurities were admitted to investigate their effects [2,9,10]). On this occasion, we had to test the ability of a stable operation of superpermeable membrane under unfavourable vacuum conditions.

3. Experimental results and discussion

3.1. Experimental observations

No permeation could be noticed when hydrogen was admitted at the upstream side with a cold atomizer. Switching on of the atomizer results in an upstream pressure drop and in a steep downstream pressure rise, with new steady-state pressure levels established with a definite transient time [11]. The new downstream pressure depends on the downstream pumping speed that is controlled with a valve (see Fig. 1) and it may be orders of magnitude higher (e.g. 10^3 times in our experiments) than the upstream pressure (i.e. *the membrane compresses the permeating gas*). Thus a steady-state *membrane pumping* due to the atomic-driven permeation is observed. Experimental data on the membrane pumping speed, S_m, and the permeation flux density, j_m, *versus* upstream pressure, p, taken at three different sets of atomizer and membrane temperature (T_a and T_m, respectively) are presented in Fig. 2. One can see that S_m reaches $\sim 10^3$ l/s, with the specific pumping speed of ~ 1 l/s *per* 1 cm^2 membrane area [1], while j_m and p reach values of 3×10^{17} atom/cm^2/s and

[1] This specific pumping speed might have been 30–40% higher [10], if there were no additional recombination losses of atomic hydrogen at the reinforced frame needed to adjust the atomizer to the plasma machine.

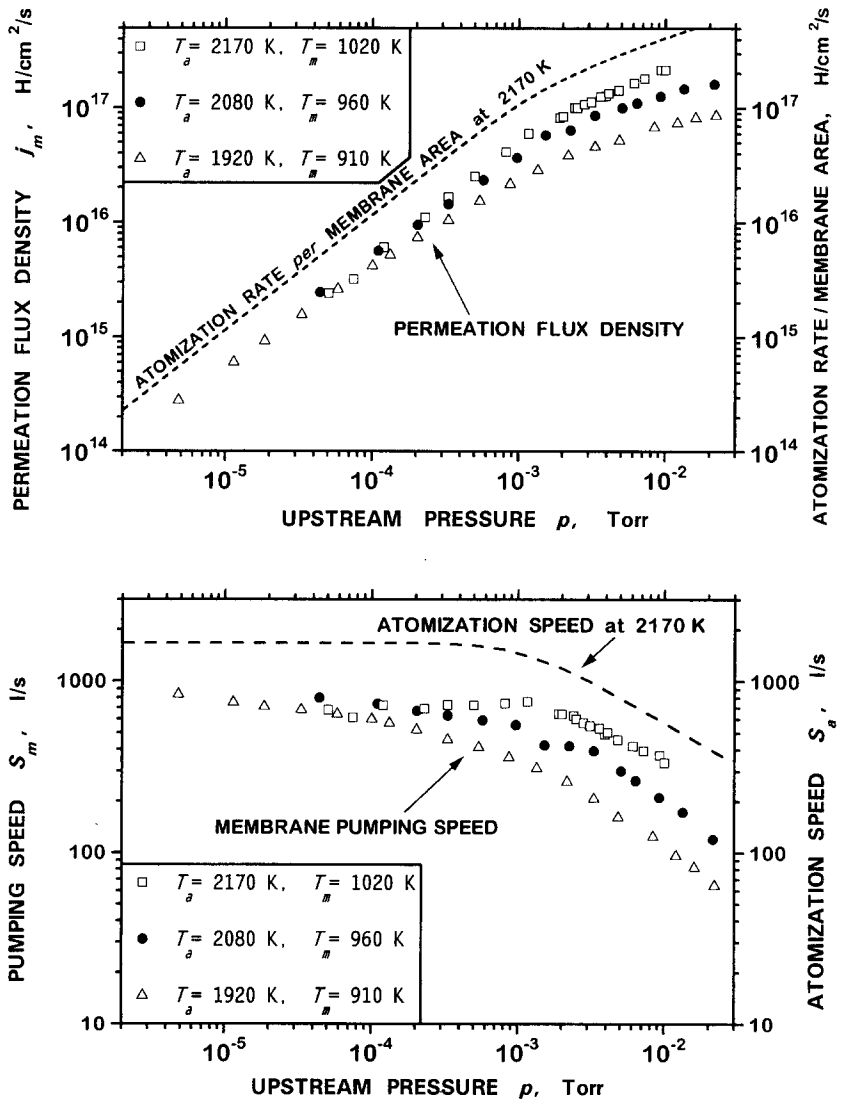

Fig. 2. Experimental dependencies on upstream pressure of the membrane pumping speed and permeation flux density at three different sets of atomizer (T_a) and membrane (T_m) temperature (membrane temperature is determined by the radiation from atomizer). The rate of atomization (in l/s) and the yield of atomic hydrogen *per* 1 cm^2 membrane area (in H atom/cm^2/s) are also presented as calculated by Eqs. (5) and (6) with the values $\alpha_{H_2} = \gamma = 0.3$.

3×10^{-2} Torr, respectively. It was only a limited capacity of the turbo-molecular pumps that prevented us advancing to higher flux densities and upstream pressures.

There are two distinctly different pressure ranges. *At relatively low upstream pressures,* S_m does not depend on p and, correspondingly, $j_m \propto p$. In this pressure range S_m and j_m depend neither on T_a nor on T_m. At higher pressures, j_m rises slower with p: $j_m \propto \sqrt{p}$ and therefore S_m starts coming down as $1/\sqrt{p}$. In contrast to the low-pressure range, S_m and j_m rapidly fall with T_a decreasing. The boundary between the two ranges moves to higher pressures with T_a rising.

3.2. Performance of a system comprising a membrane and an atomizer

The constant S_m against changes in p and T_m is typical for the range of relatively low pressures (permeation fluxes) investigated previously [5,6,10,11,15] and that is an intrinsic characteristic of superpermeability [1,2,6]. Still it was particularly important for us to understand what happens at higher pressures and flux densities where a decrease in S_m was observed. Thus, it was necessary to analyze the roles of the atomizer and the membrane separately.

Assuming that the membrane area substantially exceeds that of the atomizer, one can express the membrane pumping speed, S_m, and the permeation flux, J_m, as follows:

$$S_m \approx S_a \cdot \delta \cdot \frac{\chi}{\alpha_H}; \qquad J_m \approx J_a \cdot \delta \cdot \frac{\chi}{\alpha_H}, \tag{2}$$

where S_a is the 'atomization speed' (viz. a volume of hydrogen at a given pressure converted into atoms *per* unit time, expressed in the same units as S_m), J_a is a full amount of atoms produced by the atomizer *per* unit time, χ is a permeation probability for an H atom impinging at the membrane surface, α_H is a sticking coefficient of an H atom at the membrane and δ is a constant 'atomic efficiency factor':

$$\delta = \frac{\alpha_H \cdot S_m}{\alpha_H \cdot S_m + \Sigma(\gamma_i S_i) + S_d}, \tag{3}$$

where $\Sigma(\gamma_i S_i)$ is the recombination losses at all surfaces except the membrane itself (S_i and γ_i are respective surface areas and H atom recombination coefficients) and S_d is an orifice area of the diaphragm through which the upstream chamber is pumped with an external pump.

At superpermeation, $\chi \approx \alpha_H$ and consequently,

$$S_m \approx S_a \cdot \delta; \qquad J_m \approx J_a \cdot \delta. \tag{4}$$

Thus S_m and J_m differ from S_a and J_a only by a constant factor δ in the superpermeation regime.

At drifting away from superpermeation (e.g. towards the so-called 'diffusion-limited' permeation regime), the ratio χ/α_H becomes effectively dependent on p and T_m [1,2,16,17] and therefore the ratios S_m/S_a and J_m/J_a should be markedly changing with p, T_m and T_a as well (T_m and T_a are interdependent in our experiment). Thus, if we find that S_m and J_m change in parallel with S_a and J_a it will be the proof that we are actually dealing with the superpermeation regime, while the pumping speed fall is due just to a lower atomizer efficiency.

3.3. Hydrogen atomization at a hot metal surface

The atomization process was investigated by many researches starting from Langmuir (e.g. Ref. [18]) as a simplest catalytic reaction. The atomization speed, S_a, and the atomization flux, J_a, may be expressed as:

$$S_a\,(\mathrm{l/s}) = 43.7 \times B_a\,(\mathrm{cm^2}) \times \beta; \qquad J_a\,(\mathrm{atom/s}) = 2 \times 43.7 \times 3.6 \cdot 10^{19} \times p\,(\mathrm{Torr}) \times B_a\,(\mathrm{cm^2}) \times \beta, \tag{5}$$

where B_a is an atomizer surface area and β is a probability of atomization of a hydrogen molecule *per* single impact on the hot surface; β can be presented [19] as follows:

$$\beta = \begin{cases} \alpha_{H_2} & \text{at } p \ll p^* \\ 19.5 \cdot \dfrac{\gamma \cdot T_a^{0.86}}{\sqrt{p}} \cdot \exp\left(-\dfrac{217\ \mathrm{kJ/mol}}{RT_a}\right) \times \sqrt[4]{293/T_a} & \text{at } p \gg p^*, \end{cases} \tag{6}$$

where

$$p^* = \left[19.5 \cdot \frac{\gamma}{\alpha_{H_2}} \cdot T_a^{0.86} \cdot \exp\left(\frac{217\ \mathrm{kJ/mol}}{RT_a}\right) \times \sqrt[4]{293/T_a}\right]^2, \tag{7}$$

α_{H_2} is a sticking coefficient of H_2 molecules, γ is a recombination coefficient of H atoms at the atomizer surface, p (Torr) is hydrogen pressure measured with a gauge at room temperature [2]. Several β isotherms at typical α_{H_2} and γ values are presented in Fig. 3.

Thus there are *two pressure ranges* to be distinguished. At *low pressures*, almost all the molecules sticking at the surface are desorbed in the form of atoms ($\beta \approx \alpha_{H_2}$). For the clean surface of transient metals, α_{H_2} does not depend on p and T_a when the surface is far from saturation with adsorbed H atoms [12] (which is always true when the upper line in Eq. (6) is valid). Hence β also does not depend on p and T_a here. In the *range of higher pressures*, only a small portion of sticking molecules is desorbed as atoms, and β obeys a law $\propto 1/\sqrt{p}$. The physical reason for the atomization probability to drop

[2] An equilibrium constant for the $H + H \leftrightarrow H_2$ reaction referring to a pressure at the *reaction temperature* was employed [18] to derive Eq. (6). The factor $\sqrt[4]{293/T_a}$ accounts for the pressure being gauged at *room temperature*.

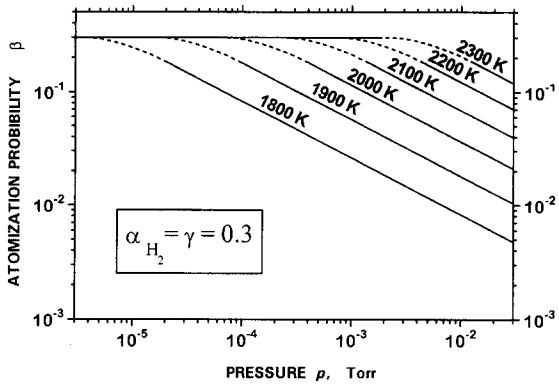

Fig. 3. Isotherms of the probability of atomization calculated according to Eq. (6) with $\alpha_{H_2} = \gamma = 0.3$ (solid lines). The dashed lines correspond to the transition between the two atomization regimes described by the upper and lower lines of the equation.

with pressure is that a higher concentration of adsorbed H atoms results in a higher probability of their coupling and desorbing as molecules. In contrast to the low-pressure range, β becomes strongly dependent on T_a: the apparent activation energy for β (217 kJ/mol) equals half the H_2 molecule binding energy.

3.4. Superpermeability regime evidences

There is a marked similarity between the atomization probability and membrane pumping speed isotherms (Figs. 2 and 3). Also presented in Fig. 2 are the atomization speed, S_a, and the atomization rate *per* unit membrane area, J_a/B_m, as calculated by Eqs. (5) and (6) at one temperature, to give a direct comparison with the experimentally measured membrane pumping speed, S_m, and permeation flux density, j_m. With reasonable α_{H_2} and γ values ($\alpha_{H_2} = \gamma = 0.3$) [12,18] taken to compute S_a and J_a, the difference between the pairs of curves: S_m and S_a, and j_m and J_a/B_m, respectively, is reduced to just a constant factor *over the whole pressure range investigated*, which proves that the membrane remains superpermeable even at higher pressures (see Section 3.2). The δ value of 0.6–0.7 also looks reasonable with regard to the losses of atoms to be anticipated in our system.

There are also other evidences to the effect that the membrane is superpermeable over the whole range of p and j_m investigated.

3.4.1. Dependence on T_a

One can see from Fig. 2 that S_m and j_m depend on atomizer temperature at higher pressures. One might associate this dependence with the temperature of the membrane rather than with that of the atomizer (since we cannot change T_a and T_m independently) and to think that the independence of permeation of T_m that is characteristic of superpermeability disappears in the high-pressure range. To check it, special measurements of S_m and j_m *versus* T_a were performed that yielded a temperature dependence close to that expected for the atomization probability, β, in this pressure range, with an apparent activation energy of 200–250 kJ/mol (see Eq. (6)). Thus we have grounds to believe that the permeation probability remains independent of T_m (and is very large) in the high-pressure range and to ascribe the observed temperature dependence to a decrease in the atomization rate and in the incident atomic flux.

3.4.2. Transient processes

We can follow the permeation flux rise and decay at a step-wise switching on and off of the gas admittance at a hot atomizer. The transient processes observed correspond to those characteristic of the superpermeation regime [1,2,6] even at the highest flux densities. Specifically, the transient permeation time, τ_p, while decreasing with the permeation flux density approximately as $\tau_p \propto 1/\sqrt{j_m}$ (typical for superpermeation), still remains much greater than the time τ_D of a single diffusion passage of an absorbed H atom across the niobium membrane even at the highest j_m investigated. E.g. at $T_m = 1020$ K and $j_m = 2 \times 10^{17}$ atom/cm^2/s, we get $\tau_p \approx 2$ s, whereas $\tau_D \approx 0.15$ s (if one takes 1.5×10^{-4} cm^2/s for the diffusion coefficient [20]). The condition $\tau_p \gg \tau_D$ means that the absorbed atoms cross the membrane many (τ_p/τ_D) times before desorption and it is actually this fact that gives rise to superpermeation (if an additional requirement is also fulfilled that the gas evolution through the downstream surface is at least no more difficult than the evolution back to the upstream side).

3.5. Physico–chemical reliability conditions

Our whole experimental campaign lasted for about 2000 h, approximately half of which was in the operational regime (T_m = 500–700°C, $p = 10^{-5}$–10^{-2} Torr, with the atomizer operating) and the other half at room temperature (at night time). The membrane was exposed to *thermal atomic* hydrogen with a peak incident flux of $\sim 10^{18}$ cm^{-2} s^{-1}, and with a total fluence during the campaign of $\sim 10^{22}$ cm^{-2}. It produced no effect on the behaviour of superpermeable membrane, similarly to what was observed earlier at much lower flux densities [3–6,10,11,15].

Moreover, the membrane and the atomizer have got an exposition to water ($\sim 10^6$ Langmuir for the whole campaign) and oil (10^5–10^6 Langmuir) vapours due to relatively poor vacuum conditions (see Section 2). Still all the characteristics of the superpermeable membrane remained quite stable and reproducible.

That means that the membrane inlet surface remains covered with a non-metal film (mainly oxides) of about *monatomic* thickness: thicker films would prevent thermal H atoms from being absorbed with such a high sticking coefficient [2,6], while the film splits or ruptures leaving parts of the metal surface bare would result in the dominance of the back desorption at upstream side. Thus, this experiment provides one more evidence that the state of the surface responsible for superpermeability is rather stable and exhibits a capability to maintain itself, if the operational temperature is not too low to bring down very low the rate of the mechanisms responsible for film restoration and replenishment [10].

4. Summary

(1) Superpermeability was observed at record parameters with reference to both: the permeation flux density of 3×10^{17} H/cm^2/s (by one order of magnitude larger than ever before) and the operational pressure of 3×10^{-2} Torr. It was only a limited capacity of the turbo-molecular pumps employed that did not permit our advancing further to still higher flux densities, though the analysis of experimental results indicates that a substantial advancement should be possible.

(2) A superpermeable Nb membrane combined with an atomizer demonstrated a reliable operation for the duration of a $\sim$ 2000 h campaign in spite of a high density of the atomic hydrogen flux and under the realistic vacuum conditions of a linear plasma device: in the presence of significant amounts of the water and oil vapours.

Acknowledgements

We thank A. Sagara, S. Yamaguchi, S. Takamura, N. Ohno, K. Morita, N. Noda and K. Akaishi for their valuable help. We also express our deep gratitude to A. Iiyoshi and A. Motojima for their interest in, and their support of, this research. The portion of this work performed in Russia was partly supported by the International Science Foundation, Grants Nos. NWM000 and NWM300.

References

[1] A.I. Livshits, Sov. Phys. Tech. Phys. 21 (1976) 187.
[2] A.I. Livshits, M.E. Notkin and A.A. Samartsev, J. Nucl. Mater. 170 (1990) 74.
[3] A.I. Livshits, Sov. Tech. Phys. Lett. 3 (1977) 236.
[4] A.I. Livshits, M.E. Notkin and S.V. Yakovlev, Sov. Tech. Phys. Lett. 4 (1978) 192.
[5] I. Ali-Khan, F. Waelbroeck, K.J. Dietz and P. Wienhold, J. Nucl. Mater. 76–77 (1978) 337.
[6] A.I. Livshits, M.E. Notkin, Yu.M. Pustovoit and A.A. Samartsev, Vacuum 29 (1979) 113.
[7] J. Park, T. Bennet, J. Schwarzmann and S.A. Cohen, J. Nucl. Mater. 220–222 (1995) 827.
[8] A.I. Livshits and M.E. Notkin, Sov. Tech. Phys. Lett. 7 (1981) 605.
[9] A.I. Livshits, M.E. Notkin, A.A. Samartsev and I.P. Grigoriadi, J. Nucl. Mater. 178 (1991) 1.
[10] A.I. Livshits, M.E. Notkin, V.I. Pistunovich, M. Bacal and A.O. Busnyuk, J. Nucl. Mater. 220–222 (1995) 259.
[11] A.I. Livshits, M.E. Notkin, A.A. Samartsev, A.O. Busnyuk, A.Yu. Doroshin and V.I. Pistunovich, J. Nucl. Mater. 196–198 (1992) 159.
[12] M.W. Roberts and C.S. McKee, Chemistry of Metal-Gas Interface (Clarendon, Oxford, 1978).
[13] G. Janeschitz et al., Proc. 15th Int. Conf. on Plasma Physics and Contr. Nucl. Fus. Res., Seville, Spain, September 26–October 1, Vienna (1994).
[14] N. Ohyabu et al., J. Nucl. Mater. 220–222 (1995) 298.
[15] V.R. Kapitansky, A.I. Livshits, I.M. Metter and M.E. Notkin, Sov. Phys. Tech. Phys. 21 (1976) 602.
[16] F. Waelbroeck, I. Ali-Khan, K.J. Dietz and P. Wienhold, J. Nucl. Mater. 85–86 (1979) 345.
[17] D.K. Brice and B.L. Doyle, J. Vac. Sci. Technol. A 5 (1987) 2311.
[18] D. Brennan, Adv. Catal. 15 (1964) 1.
[19] A.I. Livshits, F. El-Balghity and M. Bacal, Plasma Source Sci. Technol. 3 (1994) 465.
[20] E. Fromm and E. Gebhardt, eds., Gase und Kohlenstoff in Metallen (Springer, Berlin, 1976).